HHS Public Access

Author manuscript

Biochem Biophys Res Commun. Author manuscript; available in PMC 2022 October 08.

Published in final edited form as:

Biochem Biophys Res Commun. 2021 October 08; 573: 145–150. doi:10.1016/j.bbrc.2021.08.033.

Adenylyl cyclase 3 regulates osteocyte mechanotransduction and primary cilium

Michael P. Duffy[1,*], **McKenzie E. Sup**[1], **X. Edward Guo**[1]

[1]Department of Biomedical Engineering, Columbia University in the City of New York

Abstract

Osteocytes are accepted as the primary mechanosensing cell in bone, but how they translate mechanical signals into biochemical signals remains unclear. Adenylyl cyclases (AC) are enzymes that catalyze the production of second messenger cyclic adenosine monophosphate (cAMP). Osteocytes display a biphasic, cAMP response to fluid shear with an initial decrease in cAMP concentrations and then an increased concentration after sustained mechanical stimulation. To date, AC6, a calcium-inhibited AC, is the primary isoform studied in bone. Since osteocytes are calcium-responsive mechanosensors, we asked if a calcium-stimulated isoform contributes to mechanotransduction. Using a transcriptomic dataset of MLO-Y4 osteocyte-like cells from the NIH Gene Expression Omnibus, we identified AC3 as the only calcium-stimulated isoform expressed. We show that inhibiting AC3 in MLO-Y4 cells results in decreased cAMP-signaling with fluid shear and increased osteogenic response to fluid flow (measured as Ptgs2 expression) of longer durations, but not shorter. AC3 likely contributes to osteocyte mechanotransduction through a signaling axis involving the primary cilium and GSK3β. We demonstrate that AC3 localizes to the primary cilium, as well as throughout the cytosol and that fluid-flow regulation of primary cilia length is altered with an AC3 knockdown. Regulation of GSK3β is downstream of the primary cilium and cAMP signaling, and with western blots we found that GSK3β inhibition by phosphorylation is increased after fluid shear in AC3 knockdown groups. Our data show that AC3 contributes to osteocyte mechanotransduction and warrants further investigation to pave the way to identifying new therapeutic targets to treat bone disease like osteoporosis.

Keywords

adenylyl cyclase 3; primary cilium; osteocyte; mechanotransduction; cAMP; Gsk3beta

[*]Corresponding Author, mpd2133@columbia.edu.

Declaration of interests

The authors declare that they have no known competing financial interests or personal relationships that could have appeared to influence the work reported in this paper.

INTRODUCTION

Adenylyl cyclases (ACs) are enzymes responsible for the conversion of adenosine triphosphate (ATP) into the second messenger cyclic adenosine monophosphate (cAMP) and they contribute to memory formation, depression, obesity, renal function, cholangiocyte bile flow detection, and bone mechanotransduction [1–7]. cAMP signaling is highly compartmentalized [8] and the differential expression and organization of the nine membrane-bound AC isoforms is important for the varied effect [9]. Activity of ACs are further regulated in an isoform-dependent fashion by calcium, calmodulin, G-proteins, and G-protein coupled receptors (GPCRs) [9]. Due to their highly regulated and multifaceted function, adenylyl cyclases offer a potent avenue for the identification of signaling systems to target for drug development. Despite this, little is known about what adenylyl cyclases contribute to osteocyte – bone's primary mechanosensing cell – function.

Bone is a highly adaptive organ, responding to increased loading with accrual of new bone, and to decreased loading with resorption of bone. The osteocyte, a full differentiated bone cell embedded in the mineral matrix, is accepted as a critical bone mechanosensing cell. In terms of AC's mechanosensing function, osteocyte research has focused primarily on the role of adenylyl cyclase 6 (AC6), because it is expressed in an osteocyte cell-line and localizes to a mechanosensitive organelle, the primary cilium [10]. *In* vitro, inhibiting AC6 results in an increased flow-induced cAMP production and decreased osteogenic response [10]. Using a global knockout mouse, loss of AC6 led to decreased load-induced bone formation. Since osteocytes are calcium-responsive mechanosensing cells [11], it is logical that a loss of AC6, a calcium inhibited isoform, would result in a loss of the initial decrease in cAMP levels with fluid flow. But after longer durations of fluid-flow, cAMP levels increase while osteocytes exhibit repeated calcium spikes [11,12]. Therefore, we hypothesized that a calcium-stimulated AC also contributes to osteocyte mechanoresponse. In fact, inspection of the NIH GSE dataset GSE70667 [13], the only calcium-stimulated isoform expressed by MLO-Y4 cells, an osteocyte-like cell line, is AC3 (see supplemental Figure 1).

AC signaling can affect osteocyte mechanotransduction through several pathways. cAMP is a potent regulator of the primary cilium, an antenna-like mechanoresponsive organelle that may be a key contributor to osteocyte function [14,15]. Cells with longer primary cilia have a greater osteogenic response to fluid shear [16] and primary cilia have a distinct cAMP pool from the cytosol [17]. Downstream of primary cilia signaling is protein kinase A (PKA), which is composed of two regulatory and two catalytic subunits. Both types of subunits come in a variety of isoforms leading to a diversity of actions [18]. Constitutively active PKA in osteocytes and mature osteoblasts results in increased bone formation rates, and enhanced cortical and trabecular bone properties [19]. Due to the diversity of PKA enzymes, studying downstream effectors, Creb and GSK3β, which are important transcriptional regulators in bone [20–22], allows us to probe this signaling cascade.

In this work we determine if the calcium-stimulated AC3 contributes to osteocyte mechanotransduction and if the primary cilium is implicated in this function. We examine this using an osteocyte-like MLO-Y4 cell line and murine histological immunostaining.

Changes in the expression levels of *Ptgs2,* encoding for a rate-limiting enzyme in the production of PGE_2, are used to quantify mechanoresponse to fluid shear application [23,24]. The goal of this work is to shed light on how adenylyl cyclases contribute to bone mechanotransduction.

MATERIALS AND METHODS

Cell Culture and AC3 siRNA-mediated knockdown

MLO-Y4 cells were cultured as described by Rosser and Bonewald [25]. Cells were plated on Type I collagen (Corning, 354236) coated dishes or glass slides. Cells were maintained in MEMalpha containing 2.5% FBS, 2.5% CS and 1% P/S (Gibco, 15140122) and passaged to limit confluence below 80%. An siRNA-mediated knockdown was used to inhibit AC3 production. Cells (1.25 million) were suspended in BTXExpress electroporation buffer with 7.5 μL of 20 μM of each of two Adcy3 siRNAs (Mss200418 and Mss200419, ThermoFisher Scientific) or 15 μL of 20 μM medium GC-content negative siRNA control (ThermoFisher Scientific, 12–935-300). The cell suspension was electroporated with a single 300 V, 100 Ω, 1000 μF pulse on ECM 630 Electroporation System (Harvard Apparatus) with 4 mm electroporation cuvette (Harvard Apparatus, 45–0126). Electroporated cells were immediately resuspended in culture medium and divided between ten large glass microscope slides (Fisher Scientific, 12250B). Culture medium was refreshed within 24 hours.

Fluid Flow Application

Dynamic fluid flow was applied with a previously described custom parallel-plate fluid-flow chamber [10,15,16]. Oscillatory fluid flow was applied at 1 Hz with a peak shear stress of 1 Pa. For gene expression quantification, flow was applied for 2, 15, 30, or 60 minutes and samples collected after a total of 60 minutes. For cAMP quantification, flow was applied for 2 or 60 minutes and samples were collected immediately after. Fluid flow was applied for one and two hours for immunostaining and western blotting, respectively. Static samples were assembled into flow chambers for an equal duration of time.

Gene expression

Total RNA was isolated using a phenol-chloroform extraction with TRI reagent (Sigma-Aldrich, 93289). RNA concentration was quantified on a NanoDrop 1000 spectrophotometer and 2 μg of RNA was used for reverse transcription with High-Capacity Reverse Transcription Kit (Applied Biosystems, 4368813). Real-time quantitative PCR was performed on cDNA using ABI Prism 7900 Sequence detection system and quantified using the standard curve method. We used Life Technologies primers for AC3 (Mm00460371_m1), PTGS2 (Mm00478374_m1) and endogenous control GAPDH (4352339E).

Immunostaining and Microscopy

Cells were washed in cold PBS and fixed with 10% neutral buffered formalin. Ulnae were dissected from 16-week-old C57BL6/J mice, fixed for 48 hours in 4% paraformaldehyde, and decalcified in 10% EDTA for two weeks. Paraffin embedding and sectioning were performed by the histology core at Columbia University Herbert Irving Comprehensive

Cancer Center. All animal use was approved by Columbia University's IACUC. Cell and tissue samples were similarly immunostained. Samples were permeabilized in 0.01% Triton X-100, and blocked with 1% w/v BSA (Sigma-Aldrich, A2058) and 10% normal goat serum (R&D Systems, S13195) in PBS (1X). Primary and secondary antibodies were diluted in blocking solution and applied for 1 hour at room temperature or overnight at 4 °C. Primary antibodies against AC3 (rabbit polyclonal, diluted 1:500, Abcam, ab175093) and acetylated alpha tubulin (mouse monoclonal from ECACC C3B9 hybridoma cell line 00020913, diluted 1:10). Secondary antibodies, Alexa Fluor 488 goat ant-mouse (Invitrogen, A11029) and Alexa Fluor 568 goat anti-rabbit (Invitrogen, A11036), were diluted 1:200. NucBlue (Invitrogen, R37606) was used as a nuclear counterstain. Samples were mounted with Prolong Gold antifade mountant (Invitrogen, P36930).

Confocal images were collected on an Olympus Fluoview FV1000 microscope with 40x UPLFLN oil immersion objective (N.A. 1.30). Images were process with the FIJI distribution of ImageJ. Maximum projection z-stacks of raw *in vitro* image data were created. Histological samples were deconvolved using plugins DeconvoleLab2 and PSFGenerator [26]. Orthogonal projections of individual osteocytes were projected for visual inspection.

For quantifying primary cilia length, images were acquired on an Olympus IX81 microscope with a U-RFL-T mercury lamp, Hammamatsu C10600–10B camera, and DAPI and GFP filter cubes. At least five images were collected from the middle third of the microscope slide using a 40x UPlan FLN 0.45 NA dry objective. Primary cilia length was measured manually using the segmented line tool in ImageJ. Measurements from each micrograph of the same flow sample were pooled and the average length calculated.

cAMP Quantification

Immediately after fluid shear, cells were washed in cold PBS, incubated in 0.1 M HCl and lysed. Samples were centrifuged at 1,000 × g for 10 minutes at 4 °C and supernatant collected. cAMP ELISA was performed according to manufacturer's instructions (Cayman Chemical, 581001) and cAMP levels were normalized to sample protein concentration (ThermoScientific Pierce BCA Protein Assay Kit, P123227).

Western Blots

After fluid shear, each slide was washed in cold PBS and protein isolated with 0.6 mL RIPA buffer (Santa Cruz Biotechnology, SC-24948) supplemented with 10 μL/mL each of PMSF, sodium orthovanadate, and protease cocktail inhibitor (Santa Cruz Biotechnology, sc-24948). Protein was concentrated using an acetone precipitation and were resuspended in 60 μL of sample buffer (26.5 mM Tris HCl, 35.25 mM Tris Base, 0.5% LDS, 0.128 mM EDTA at a pH of 8.5 supplemented with 5 μL/mL each of PMSF, sodium orthovanadate, and protease cocktail inhibitor). Protein concentration was determined as for cAMP ELISA. The NuPage XCell II system was used for running the gel electrophoresis of 15 μg of reduced samples on a NuPAGE Novex 4–12% Bis-Tris Gel (Fisher Scientific, NP0321) and blot transfer to PVDF paper (Invitrolon, Fisher Scientific, LC2005). Gel electrophoresis was run at 200 V with MOPS running buffer (NP0001)

until the loading dye reached the bottom of the gel (about 50 minutes) with WesternC Precision Plus Protein Ladder (Bio-Rad, 161–0385). Gel transfer was performed at room temperature for one hour at 30 V. Blots were blocked in 5% nonfat dry milk (Bio-Rad, 170–6404) in tris buffered saline (Fisher, BP-2471) with 0.1% Tween20 (Fisher, BP337). Primary incubation was conducted overnight in 1% nonfat dry milk solution. Primary antibodies were phospho-CREB (1:600, Invitrogen, PIPA585645), Creb1 (1:750, ProteinTech, 12208–1-AP), phospho-GSK3β (1:1000, ProteinTech, 14850–1-AP), GSK3β (1:1000, ProteinTech, 22104–1-AP), and GAPDH (1:10,000, ProteinTech, 60004–1-lg). Secondary antibodies were HRP-goat anti-mouse (ProteinTech SA00001–1), HRP-goat anti-rabbit (ProteinTech SA00001–2), and StrepTactin HRP-conjugate (0.33 μL/10 mL, Bio-Rad, 1610380). Enhanced chemiluminescence detection was performed (Clarity ECL, Bio-Rad 170–5061) and imaged on a FujiFilm LAS-4000 system. Images were analyzed in ImageJ to quantify the intensity of each band after background subtraction and normalization to GAPDH.

Statistical Analysis

Data are represented as mean ± standard error measure. Statistical analysis was carried out in GraphPad Prism 5. One-way ANOVA was used to determine if there was a significant difference between the means followed by Bonferroni's multiple comparison test. One-way two-sided student T-tests were used to determine if flow/static or knockdown/control normalized samples were significantly different from 1. Statistical significance was determined at $\alpha = 0.05$.

RESULTS

AC3 contribution to MLO-Y4 mechanosensing

AC3 expression levels were reduced by 45% after siRNA-mediated knockdown (Figure 1A). *Ptgs2* expression, a measure of osteogenic response to fluid shear, was unchanged with AC3 knockdown (Figure 1B) in static samples. There was no difference between control and AC3-knockdown groups in static normalized *Ptgs2* expression at 2, 15, and 30 minutes of fluid shear (Figure 1C). After 60 minutes, there was a significant increase in the flow-induced fold-increase of *Ptgs2* expression in AC3-knockdown samples (3.73 ± 0.27) compared to controls (2.59 ± 0.19).

cAMP Response to fluid shear

In static conditions, cAMP concentration (pmol cAMP/microgram total protein) was 0.24 ± 0.05 for control and 0.14 ± 0.03 for AC3 KD samples. While lower for AC3 KD, this was not statistically significant. Fold-change in cAMP levels after 2 minutes of fluid shear remained suppressed in AC3 KD (0.42 ± 0.14) compared to controls (0.79 ± 0.15) and was statistically lower after 60 minutes with an AC3 KD group fold-decrease of 0.29 ± 0.08, and a control group fold-increase of 1.19 ± 0.33.

AC3 localizes to the osteocyte primary cilium and regulates length

Immunostaining revealed that AC3 localizes to the primary cilium, as well as throughout the cytosol, in MLO-Y4 cells and osteocytes in murine long bone (Figure 3A), indicating it can

contribute to both cytosolic and ciliary cAMP pools. Primary cilia lengths were measured in static conditions and after one hour of dynamic fluid flow. There was no difference in length between statically cultured control -- 1.39 ± 0.09 μm – and AC3 KD – 1.48 ± 0.08 μm – samples (Figure 3B). With fluid flow, the primary cilium length shortened by about 20% with an AC3 knockdown, while there was no significant change in the control group (Figure 3C).

Activation of downstream cAMP targets

Activation of Creb and GSK3β were investigated as downstream targets of cAMP and primary cilia signaling (Figure 4). Between static and flow samples for both control and AC3 KD groups, there was no significant difference in Creb expression, though the AC3 KD group had a greater variance. With flow there was a significant increase in phosphorylated Creb in the control group and was just beyond the threshold for significance in the AC3 KD group ($p = 0.066$), but between groups there was no difference. Total GSK3β protein content increased with fluid flow in the AC3 KD group, and was significantly different than the levels in control flow cells. Since the total amount of GSK3β varied between groups, phosphorylated GSK3β was normalized to GAPDH. With dynamic flow, we found a significantly higher level of GSK3β phosphorylation in AC3 knockdown samples, but neither control nor knockdown flow-to-static normalized phosphorylation was statistically different from unity.

DISCUSSION

We found that AC3, as a calcium-stimulated AC in a highly calcium-responsive mechanosensing cell, acts to down-regulate mechanoresponse to dynamic flow of a longer duration. Overall, cytosolic cAMP was reduced with an AC3 mRNA knockdown, regardless of mechanical stimulation. There was also a flow-induced decrease in the knockdown group primary cilia length, which is highly regulated by cAMP. It is unclear what sub-cellular pool of cAMP AC3 is responsible, but we found that AC3 localizes both to the primary cilium and cell body.

One possible way AC3 could down-regulate osteogenic signaling is by inhibiting GSK3β through the action of PKA. Although GSK3β levels increased with flow with an AC3 knockdown, GSK3β phosphorylation was also significantly increased. Because GSK3β leads to the degradation of β-catenin, its inhibition by phosphorylation would allow β-catenin to accumulate in the nucleus, and cause an upregulation of osteogenic signaling [27]. β-catenin signaling has been implicated in bone cell mechanotransduction [24] and osteogenic differentiation [28]. In addition, Ift88, critical for primary cilia formation, is shown to regulate β-catenin activity in the growth plate [29]. The primary cilium, AC3, GSK3β and β-catenin may form a potent osteogenic signaling axis.

One limitation of this work is that the AC3 mRNA knockdown was modest (45%). Despite this there were significant effects of AC3 on osteocyte mechanosensing that may become more apparent with a more efficient inhibition. AC3 is amenable to CRISPR/Cas9 deletion [30] and an AC3-floxed mouse for use in a Cre-Lox system has been developed [31]. This

work motivates future studies utilizing these tools to fully understand AC3 contribution to bone cell mechanobiology.

Compared to GSK3β, we found no change in Creb expression or phosphorylation with an AC3 KD, despite a reduction in cAMP levels. Creb phosphorylation was observed in porcine kidney cells after persistent elevation in cAMP signaling [32]. It is possible that Creb phosphorylation is AC3 independent or that the knockdown was insufficient to alter this role of AC3. Only control samples had a statistically significant increase in Creb phosphorylation compared to static conditions, so a potential role of AC3 in Creb mechanoregulation cannot be ruled out.

Understanding ACs role in bone biology provides a promising pathway to develop new therapeutics, but targeting ACs directly is not likely due to their diverse roles. While this study suggests an osteogenic potential of inhibiting AC3, its inhibition in other contexts has been linked with decreased memory formation [7], anosia [33], depression-like symptoms [2], and weight gain [34]. AC activity is highly regulated and dependent on co-localization with other proteins, like GPCRs. GPCRs offer a more diverse landscape to target therapeutically, and may limit off-target complications. Therapeutics targeting GPCRs represent a large proportion (about 34%) of all FDA-approved agents [35]. Furthermore, in osteocytes, the loss of the G-protein stimulatory subunit, $G_{s\alpha}$, results in osteopenia [36], indicating this is a viable path to develop a new therapeutic target for osteoporosis. Discovering which ACs are critical for osteocyte mechanobiology and identifying what GPCRs they colocalize with will narrow the pool of potential therapeutic targets.

Supplementary Material

Refer to Web version on PubMed Central for supplementary material.

ACKNOWLEDGEMENTS

The work was supported by the National Institutes of Health R01AR062177. The authors would like to give a special thanks to Dr. Christopher Jacobs, who contributed to the initial study concept, but passed away prior to the final completion.

REFERENCES

1. Blanchard MG, Kittikulsuth W, Nair AV, Baaij JH F de, Latta F, Genzen JR, et al.Regulation of Mg2+ Reabsorption and Transient Receptor Potential Melastatin Type 6 Activity by cAMP Signaling. JASN. 201576;ASN.2014121228.
2. Chen X, Luo J, Leng Y, Yang Y, Zweifel LS, Palmiter RD, et al.Ablation of Type III Adenylyl Cyclase in Mice Causes Reduced Neuronal Activity, Altered Sleep Pattern, and Depression-like Phenotypes. Biological Psychiatry. 2016121;80(11):836–48. [PubMed: 26868444]
3. Kittikulsuth W, Stuart D, Hoek ANV, Stockand JD, Bugaj V, Mironova E, et al.Lack of an effect of collecting duct-specific deletion of adenylyl cyclase 3 on renal Na^+ and water excretion or arterial pressure. American Journal of Physiology - Renal Physiology. 2014315;306(6):F597–607. [PubMed: 24431204]
4. Lee KL, Hoey DA, Spasic M, Tang T, Hammond HK, Jacobs CR. Adenylyl cyclase 6 mediates loading-induced bone adaptation in vivo. The FASEB Journal. 201431;28(3):1157–65. [PubMed: 24277577]

5. Masyuk AI, Gradilone SA, Banales JM, Huang BQ, Masyuk TV, Lee S-O, et al.Cholangiocyte primary cilia are chemosensory organelles that detect biliary nucleotides via P2Y12 purinergic receptors. Am J Physiol Gastrointest Liver Physiol. 200810;295(4):G725–34. [PubMed: 18687752]
6. Qiu L, LeBel RP, Storm DR, Chen X. Type 3 adenylyl cyclase: a key enzyme mediating the cAMP signaling in neuronal cilia. International journal of physiology, pathophysiology and pharmacology. 2016;8(3):95.
7. Wang Z, Phan T, Storm DR. The Type 3 Adenylyl Cyclase Is Required for Novel Object Learning and Extinction of Contextual Memory: Role of cAMP Signaling in Primary Cilia. J Neurosci. 2011413;31(15):5557–61. [PubMed: 21490195]
8. Moore BS, Stepanchick AN, Tewson PH, Hartle CM, Zhang J, Quinn AM, et al.Cilia have high cAMP levels that are inhibited by Sonic Hedgehog-regulated calcium dynamics. PNAS. 20161115;113(46):13069–74. [PubMed: 27799542]
9. Cooper DMF, Crossthwaite AJ. Higher-order organization and regulation of adenylyl cyclases. Trends in Pharmacological Sciences. 20068;27(8):426–31. [PubMed: 16820220]
10. Kwon RY, Temiyasathit S, Tummala P, Quah CC, Jacobs CR. Primary cilium-dependent mechanosensing is mediated by adenylyl cyclase 6 and cyclic AMP in bone cells. The FASEB Journal. 201081;24(8):2859–68. [PubMed: 20371630]
11. Morrell AE, Brown GN, Robinson ST, Sattler RL, Baik AD, Zhen G, et al.Mechanically induced Ca 2+ oscillations in osteocytes release extracellular vesicles and enhance bone formation. Bone Res. 2018319;6(1):1–11. [PubMed: 29423330]
12. Lewis KJ, Frikha-Benayed D, Louie J, Stephen S, Spray DC, Thi MM, et al.Osteocyte calcium signals encode strain magnitude and loading frequency in vivo. PNAS. 20171031;114(44):11775–80. [PubMed: 29078317]
13. Govey PM, Kawasawa YI, Donahue HJ. Mapping the osteocytic cell response to fluid flow using RNA-Seq. Journal of Biomechanics. 20151216;48(16):4327–32. [PubMed: 26573903]
14. Hoey DA, Downs ME, Jacobs CR. The mechanics of the primary cilium: An intricate structure with complex function. Journal of Biomechanics. 20121;45(1):17–26. [PubMed: 21899847]
15. Malone AM, Anderson CT, Tummala P, Kwon RY, Johnston TR, Stearns T, et al.Primary cilia mediate mechanosensing in bone cells by a calcium-independent mechanism. Proceedings of the National Academy of Sciences. 2007;104(33):13325–30.
16. Spasic M, Jacobs CR. Lengthening primary cilia enhances cellular mechanosensitivity. Eur Cell Mater. 2017220;33:158–68. [PubMed: 28217833]
17. Truong ME, Bilekova S, Choksi SP, Li W, Bugaj LJ, Xu K, et al.Vertebrate cells differentially interpret ciliary and extraciliary cAMP. Cell. 2021527;184(11):2911–2926.e18. [PubMed: 33932338]
18. Bauman AL, Scott JD. Kinase- and phosphatase-anchoring proteins: harnessing the dynamic duo. Nat Cell Biol. 20028;4(8):E203–6. [PubMed: 12149635]
19. Kao RS, Abbott MJ, Louie A, O'Carroll D, Lu W, Nissenson R. Constitutive protein kinase A activity in osteocytes and late osteoblasts produces an anabolic effect on bone. Bone. 20138;55(2):277–87. [PubMed: 23583750]
20. Armstrong VJ, Muzylak M, Sunters A, Zaman G, Saxon LK, Price JS, et al.Wnt/β-Catenin Signaling Is a Component of Osteoblastic Bone Cell Early Responses to Load-bearing and Requires Estrogen Receptor a. J Biol Chem. 2007713;282(28):20715–27. [PubMed: 17491024]
21. Nesbitt RSA, Macione J, Debroy A, Kotha SP. Bone generation through mechanical loading. World Academy of Science, Engineering and Technology. 2009;58:125–7.
22. Zhang Z-R, Leung WN, Li G, Kong SK, Lu X, Wong YM, et al.Osthole Enhances Osteogenesis in Osteoblasts by Elevating Transcription Factor Osterix via cAMP/CREB Signaling In Vitro and In Vivo. Nutrients. 20176;9(6):588.
23. Ajubi NE, Klein-Nulend J, Nijweide PJ, Vrijheid-Lammers T, Alblas MJ, Burger EH. Pulsating Fluid Flow Increases Prostaglandin Production by Cultured Chicken Osteocytes—A Cytoskeleton-Dependent Process. Biochemical and Biophysical Research Communications. 199685;225(1):62–8. [PubMed: 8769095]

24. Kamel MA, Picconi JL, Lara-Castillo N, Johnson ML. Activation of β-catenin signaling in MLO-Y4 osteocytic cells versus 2T3 osteoblastic cells by fluid flow shear stress and PGE2: Implications for the study of mechanosensation in bone. Bone. 201011;47(5):872–81. [PubMed: 20713195]
25. Rosser J, Bonewald LF. Studying Osteocyte Function Using the Cell Lines MLO-Y4 and MLO-A5. In: Bone Research Protocols. Humana Press, Totowa, NJ; 2012. p. 67–81. (Methods in Molecular Biology).
26. Sage D, Donati L, Soulez F, Fortun D, Schmit G, Seitz A, et al.DeconvolutionLab2: An open-source software for deconvolution microscopy. Methods. 20172;115:28–41. [PubMed: 28057586]
27. Beurel E, Grieco SF, Jope RS. Glycogen synthase kinase-3 (GSK3): Regulation, actions, and diseases. Pharmacology & Therapeutics. 201541;148:114–31. [PubMed: 25435019]
28. Arnsdorf EJ, Tummala P, Jacobs CR. Non-Canonical Wnt Signaling and N-Cadherin Related β-Catenin Signaling Play a Role in Mechanically Induced Osteogenic Cell Fate. Bergmann A, editor. PLoS ONE. 2009429;4(4):e5388. [PubMed: 19401766]
29. Chang C-F, Serra R. Ift88 regulates Hedgehog signaling, Sfrp5 expression, and β-catenin activity in post-natal growth plate. J Orthop Res. 20133;31(3):350–6. [PubMed: 23034798]
30. Soto-Velasquez M, Hayes MP, Alpsoy A, Dykhuizen EC, Watts VJ. A Novel CRISPR/Cas9-Based Cellular Model to Explore Adenylyl Cyclase and cAMP Signaling. Mol Pharmacol. 201891;94(3):963–72. [PubMed: 29950405]
31. Zhang Z, Yang D, Zhang M, Zhu N, Zhou Y, Storm DR, et al.Deletion of Type 3 Adenylyl Cyclase Perturbs the Postnatal Maturation of Olfactory Sensory Neurons and Olfactory Cilium Ultrastructure in Mice. Front Cell Neurosci. 2017;11. [PubMed: 28217083]
32. Jiang J, Kuo I, Abi-Jaoude J, Lemos F, Yang Y, Curci S, et al.Persistent cAMP Signaling via Vasopressin V2 Receptors Imaged in 3D Cultures Using Lightsheet Microscopy. FASEB J. 201541;29(1 Supplement):LB632.
33. Wong ST, Trinh K, Hacker B, Chan GCK, Lowe G, Gaggar A, et al.Disruption of the Type III Adenylyl Cyclase Gene Leads to Peripheral and Behavioral Anosmia in Transgenic Mice. Neuron. 20009;27(3):487–97. [PubMed: 11055432]
34. Pitman JL, Wheeler MC, Lloyd DJ, Walker JR, Glynne RJ, Gekakis N. A Gain-of-Function Mutation in Adenylate Cyclase 3 Protects Mice from Diet-Induced Obesity. PLOS ONE. 20141016;9(10):e110226. [PubMed: 25329148]
35. Hauser AS, Attwood MM, Rask-Andersen M, Schiöth HB, Gloriam DE. Trends in GPCR drug discovery: new agents, targets and indications. Nat Rev Drug Discov. 201712;16(12):829–42. [PubMed: 29075003]
36. Fulzele K, Dedic C, Lai F, Bouxsein M, Lotinun S, Baron R, et al.Loss of Gsa in osteocytes leads to osteopenia due to sclerostin induced suppression of osteoblast activity. Bone. 2018121;117:138–48. [PubMed: 30266511]

HIGHLIGHTS

- AC3 is the only calcium-stimulated adenylyl cyclase isoform osteocytes express.
- Inhibition of AC3 leads to untampered osteocyte mechanoresponse.
- Inhibition of AC3 reduces cAMP production in response to fluid shear.
- AC3 localizes to the primary cilium *in vitro* and *in vivo*.
- AC3 contributes to fluid shear regulation of primary cilia and GSK3beta.

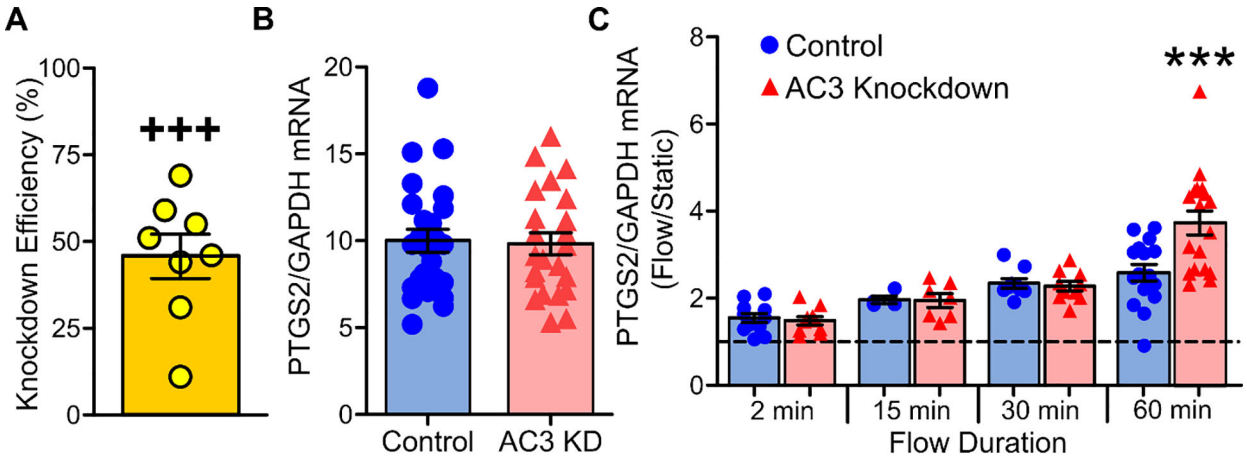

Figure 1:

AC3 inhibition results in increased osteogenic response to fluid shear. (A) AC3 knockdown resulted in a significant decrease in gene expression (N=7 experimental repeats with an average knockdown created from 3–4 control and knockdown samples per experiment). (B) In static samples, Ptgs2 gene expression is unchanged. (C) Dynamic fluid-flow resulted in an increased expression of *Ptgs2* in the AC3 KD group relative to controls only after 60 minutes of flow (C). Statistical analysis included a one-sample t-test (A), unpaired t-test (B), and 1-way ANOVA followed by Bonferroni's multiple comparison test (C). +++ $p < 0.001$. *** $p < 0.001$ compared to control of same flow duration. N = 6–11 from three experimental repeats for 2, 15, and 30 minutes of flow, and N = 16–18 from four experimental repeats for 60 minutes of flow.

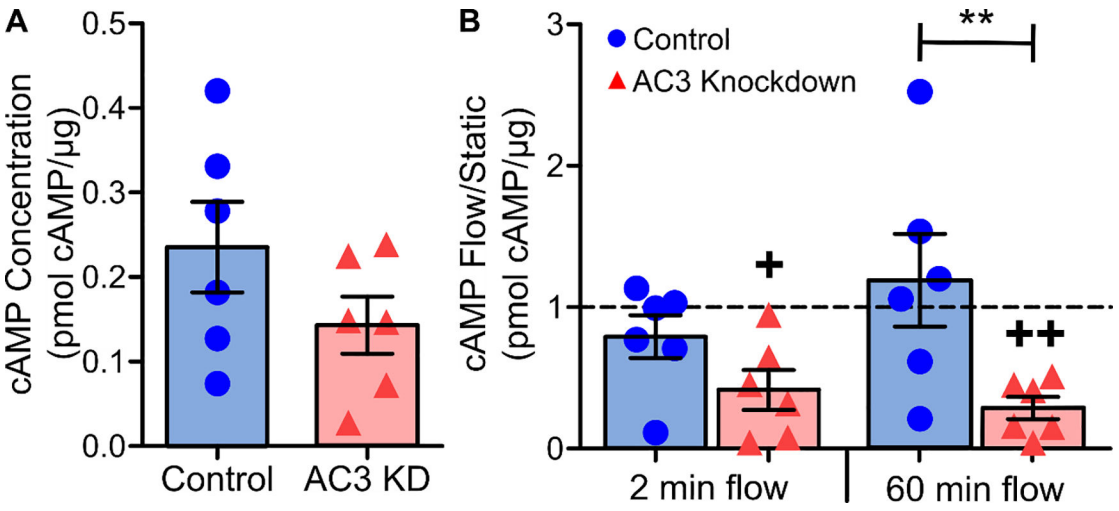

Figure 2:

cAMP levels are reduced with an AC3 knockdown. (A) Static cAMP levels, while diminished in AC3 knockdown samples, were not statistically different from control. (B) After fluid flow application, static normalized flow samples were lower in AC3 knockdown samples, though only significantly reduced after 60 minutes of fluid flow. N=6 samples. Data analysis included a t-test (A) and 1-way ANOVA followed by Bonferroni's multiple comparison. ** $p < 0.01$ between control and AC3 KD. + $p < 0.05$ and ++ $p < 0.01$ for one-sample t-test of flow/static normalized cAMP levels compared to one (i.e. no change with flow).

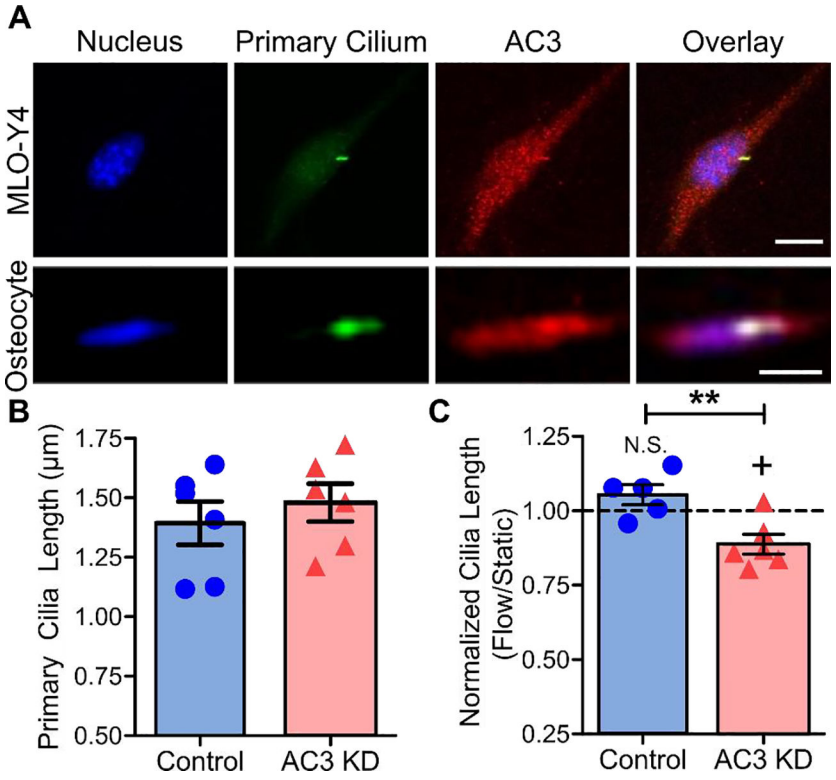

Figure 3:

AC3 localizes to the primary cilium and contributes to flow-induce ciliary regulation. (A) Immunostaining revealed that AC3 localizes to the primary cilium in MLO-Y4 cells and murine long-bone osteocytes. NucBlue was used to stain the nucleus. Anti-acetylated alpha-tubulin marked the primary cilium and an anti-AC3 antibody was used to detect AC3 localization. *In vitro* images are confocal maximum projections and *in vivo* images are maximum projections from deconvolved confocal microscopy data. Scalebar = 5 μm. (B) Static primary cilia length is similar between control and AC3 knockdown groups. (C) Primary cilia shorten with flow in knockdown cells, while there is no significant change in control. N = 6. **p< 0.01 between experimental groups. + p < 0.05 for one-sample t-test of flow/static normalized length to one (i.e. no change with flow).

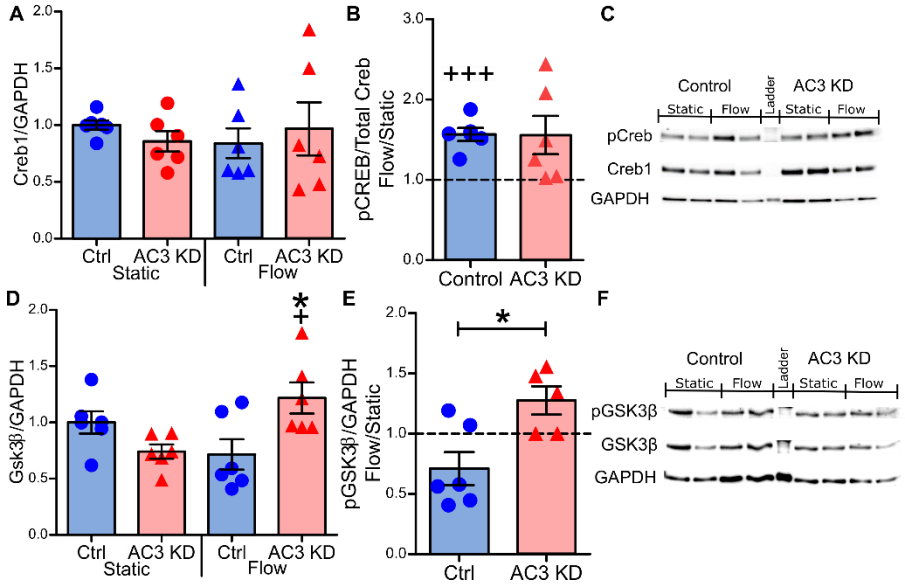

Figure 4:

Loss of AC3 alters GSK3β regulation (A) There was no difference in the total content of Creb, but there was greater variance in the AC3 KD group. (B) Flow caused a significant increase in Creb phosphorylation in the control group (+++ $p < 0.001$), but not with a knockdown ($p = 0.066$). (D) There was no difference in the total Gsk3β content in static samples, but with flow the amount of GSK3β increased in the knockdown group (* $p < 0.05$ from control flow. + $p < 0.05$ from AC3 KD static). (E) Flow-induced fold-change in GSK3β-phosphorylation was not affected by flow application, but was significantly different with AC3 KD (* $p < 0.05$). One-way ANOVA followed by Bonferroni Multiple comparison tests were performed. One-sample two-sided t-test were performed on static-normalized flow data with a theoretical mean of one. Data (N = 5–6) are from three independent experiments with one western blot shown (C,F). Full blots are shown in supplemental material.